

Figure 1.

Avocatin B is selectively toxic toward AML cells. **A**, left, a screen of a natural health product library identified avocatin B as the most potent compound at reducing TEX leukemia cell viability. Cells were incubated with compounds for 72 hours and cell growth and viability were measured by the MTS assay. Arrow, avocatin B. Inset, avocatin B's structure (21). **B**, avocatin B's activity was tested in PBSCs ($n = 4$) isolated from G-CSF-stimulated donors or cells isolated from AML patients ($n = 6$). Primary cells were treated with increasing avocatin B concentrations for 72 hours and viability was measured by the Annexin V/PI assay and flow cytometry. Data, \log_{10} EC₅₀ values. **C**, left, primary AML ($n = 3$) and normal ($n = 3$) cells were cultured with avocatin B (3 $\mu\text{mol/L}$) for 7 to 14 days and clonogenic growth was assessed by enumerating colonies as described in Materials and Methods. Data, percentage of clonogenic growth compared with control \pm SEM, similar to previously described (1). Experiments were performed twice in triplicate. Right, AML cells from one patient were treated with avocatin B (3 $\mu\text{mol/L}$) or a vehicle control for 48 hours and then intraperitoneally injected into sublethally irradiated, CD122-treated NOD/SCID mice ($n = 10/\text{group}$). After 6 weeks, human AML cells (CD45⁺/CD19⁻/CD33⁺) in mouse bone marrow were detected by flow cytometry. **, $P < 0.01$; ***, $P < 0.001$.

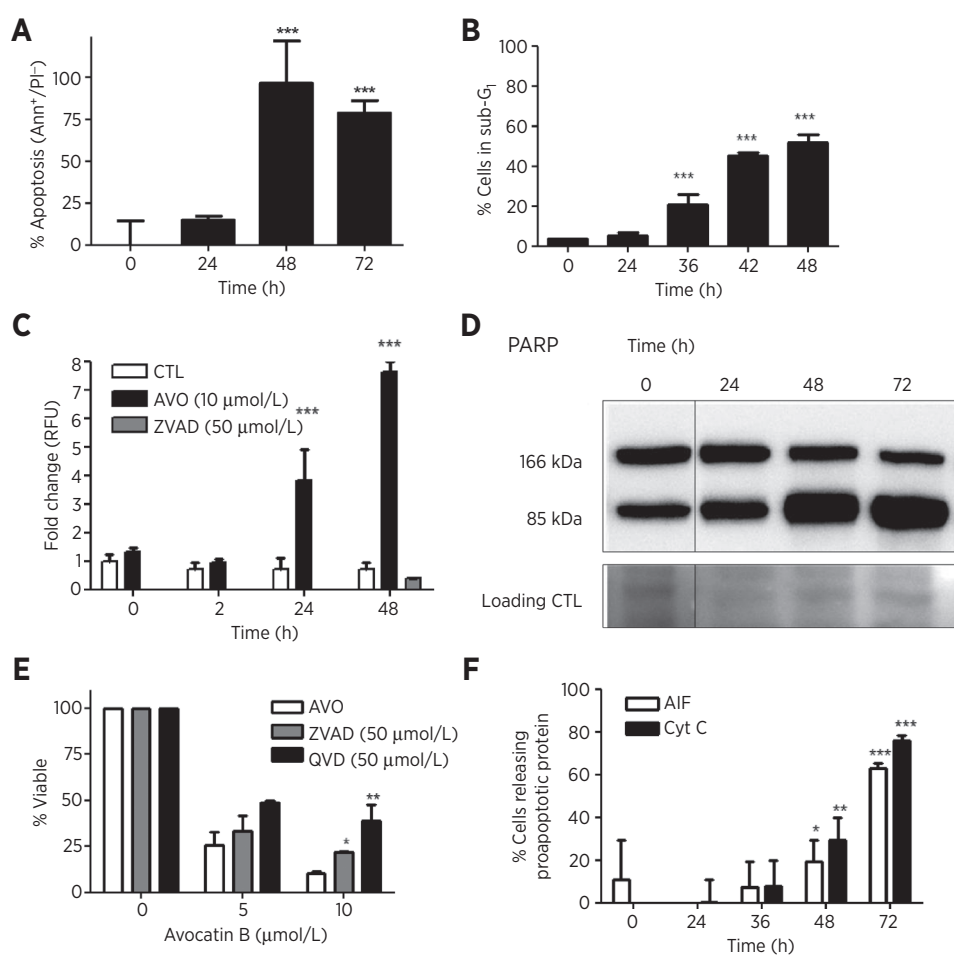
NADH, which fuels oxidative phosphorylation, and NADPH, which is an important cofactor that participates in catabolic processes during cell proliferation (23) and can also regenerate the oxidized form of GSH (e.g., GSSG) to produce reduced GSH—an important intracellular and mitochondrial antioxidant (Fig. 3A; refs. 24, 25). To test the effects of avocatin B on fatty acid oxidation, we measured mitochondrial bioenergetics of TEX cells preincubated with avocatin B or palmitate in the absence or presence of etomoxir by measuring the change in maximum oxygen consumption following oligomycin and CCCP treatment and prior to the addition of antimycin and rotenone, as previously described (11). As expected, treatment with palmitate increased the OCR, consistent with oxidation of exogenous fatty acid substrates and this increase was blocked by treatment with etomoxir, a CPT1 inhibitor (Fig. 3B and C). Similarly, avocatin B reduced palmitate oxidation, demonstrating that avocatin B inhibits the oxidation of exogenous fatty acids (Fig. 3B and C; $F_{5,17} = 40.83$; $P < 0.05$; arrows indicate when oligomycin, CCCP, and antimycin/rotenone were added). Future studies are needed to further determine the nature of CPT1's preference for avocatin B over palmitate.

Inhibiting fatty acid oxidation results in reduced NAD, NADPH, and GSH and elevated ROS

Inhibiting fatty acid oxidation can decrease NAD, NADPH, and GSH and subsequently decrease antioxidant capabilities (26). Thus, we tested the effect of avocatin B on NAD, NADPH,

and GSH levels in leukemia cells. Avocatin B (10 $\mu\text{mol/L}$), similar to etomoxir (100 $\mu\text{mol/L}$), decreased NADPH, an effect that occurred even in the presence of palmitate (175 $\mu\text{mol/L}$; Fig. 4A; $F_{9,19} = 5.129$; $P < 0.05$). Similarly, avocatin B decreased NADH and GSH (Fig. 3D: NAD: $F_{3,11} = 5.145$; $P < 0.05$; Fig. 4B: GSH: $F_{4,14} = 188.9$; $P < 0.001$).

Inhibition of fatty acid oxidation can reduce NADPH and GSH, leading to reduced antioxidant capacity, elevated ROS, and cell death (26). ROS levels were tested in avocatin B-treated cells using DCFH-DA and DHE, which measure general oxidizing species such as ROS and superoxide, respectively. TEX or primary AML cells treated with avocatin B had a time-dependent increase in ROS levels as measured by DCFH-DA (Fig. 4C, left; $F_{5,11} = 176.7$; $P < 0.01$; see Supplementary Fig. S4 for histogram data) and DHE ($F_{5,11} = 36.75$; $P < 0.01$; Fig. 4C; see Supplementary Fig. S4 for histogram data). To test the importance of ROS in avocatin B-induced death, we coincubated cells with NAC and α -tocopherol (α -Toc). NAC can neutralize a number of oxidizing species, including ROS directly or indirectly through antioxidant regeneration [i.e., convert oxidized GSH (i.e., GSSG) to reduced GSH; GSH is decreased following NADPH depletion; ref. 26] and α -Toc is a lipid-based antioxidant that accumulates in organelle membranes, particularly mitochondria, to prevent lipid peroxyl radicals formed by ROS-induced membrane damage (27). Coincubation with NAC (Fig. 4D: $F_{3,7} = 70.55$, $P < 0.05$; Fig. 4E: $F_{3,10} = 70.55$, $P < 0.05$) or α -Toc (Fig. 4D; $F_{3,7} = 10.23$; $P < 0.05$)

**Figure 2.**

Avocatin B induces mitochondria-mediated apoptosis. A and B, TEX cells were treated with 10 $\mu\text{mol/L}$ avocatin B for increasing duration and phosphatidylserine exposure in live cells (i.e., apoptotic phenotype; ANN⁺/PI⁻; A) and DNA fragmentation (B) was measured by flow cytometry. Data, fold change in apoptotic phenotype and percentage of cells in sub-G₁ peak, respectively. C and D, TEX cells were treated with 10 $\mu\text{mol/L}$ avocatin B for increasing duration and caspase-3 and -7 activation (C) and cleavage of PARP, a substrate of caspase-3, was measured by a commercially available activation assay and Western blotting (D), respectively. E, TEX cells were treated with 10 $\mu\text{mol/L}$ avocatin B in the presence and absence of the pan-caspase inhibitor Z-VAD-FMK (ZVAD) or the caspase-3-specific inhibitor Q-VD-OPh (QVD). Viability was measured after a 72-hour incubation period by the MTS assay. Data, percentage change in viability compared with controls \pm SD. F, TEX cells were treated with 10 $\mu\text{mol/L}$ avocatin B for increasing duration and cytochrome c and AIF release was measured in cytoplasmic fractions by flow cytometry. Data, percentage of cells releasing cytochrome c or AIF \pm SD. All experiments were performed three times in triplicate, and representative figures are shown. *, $P < 0.05$; **, $P < 0.01$; ***, $P < 0.001$.

abolished avocatin B-induced death. Daunorubicin was used as a negative control, as antioxidants do not protect against its cytotoxicity (28, 29). Finally, we coinubated cells with polyethylene glycol-superoxide dismutase (PEG-SOD), an antioxidant that reduces cellular concentrations of the superoxide anion. Coincubation with PEG-SOD similarly reduced ROS and blocked avocatin B's activity (Supplementary Fig. S5). Together, these results demonstrate that avocatin B decreased levels of NAD, NADPH, and GSH and that ROS is functionally important for avocatin B's activity.

Mitochondria and CPT1 are functionally important for avocatin B-induced death

We demonstrated that avocatin B inhibits fatty acid oxidation and induces apoptosis characterized by the release of mitochondrial proteins cytochrome *c* and AIF. Because avocatin B is a lipid and leukemia cells possess mitochondrial and metabolic alterations that result in their dependence on fatty acid substrates for survival (2), we hypothesized that avocatin B's toxicity was related to its localization in mitochondria. To first test avocatin B's reliance on mitochondria for cytotoxicity, we generated leukemia cells lacking functional mitochondria by culturing Jurkat-T cells in media supplemented with 50 ng/mL of ethidium bromide, 100 mg/mL sodium pyruvate, and 50 $\mu\text{g/mL}$ uridine, as previously described (30, 31). Following 60 days of passaging only live cells, the presence of mitochondria were tested by flow cytometry

following 10-nonyl acridine orange (NAO) staining and by Western blotting for mitochondrial specific proteins ND1 and adenine nucleotide translocator (ANT). The significant reduction of mitochondria was confirmed, as cells cocultured in ethidium bromide containing media demonstrated a drastic reduction in NAO staining (Supplementary Fig. S6), absence of mitochondrial respiration (Supplementary Fig. S6), and a near absence of ND1 and ANT (Fig. 5A). Avocatin B's toxicity was abolished in cells lacking functional mitochondria (i.e., JURK-Rho(0) cells), as measured by the Annexin V/PI assay (Fig. 5B; $F_{2,12} = 6.509$; $P < 0.001$). Highlighting the utility of these cells in assessing mitochondrial participation in drug activity, we have previously shown that cells lacking mitochondria were equally sensitive to their mitochondria containing controls when subjected to a compound that activates mitochondria-independent, calpain-mediated apoptosis (10).

To directly examine whether avocatin B accumulated into mitochondria, LC/MS was performed on mitochondria and cytosolic fractions of avocatin B or vehicle control-treated TEX cells. Fraction purity was confirmed by Western blot analysis of the mitochondria-specific protein ND1 (Fig. 5C; Supplementary Fig. S8). Avocatin B was detected in mitochondrial and cytosolic fractions of avocatin B-treated TEX cells (Fig. 5D). Two peaks [with a mass/charge (m/z) ratio of 285.24242 and 287.25807] were detected, which reflect the nature of avocatin B's two-lipid composition. Importantly, retention times (min)

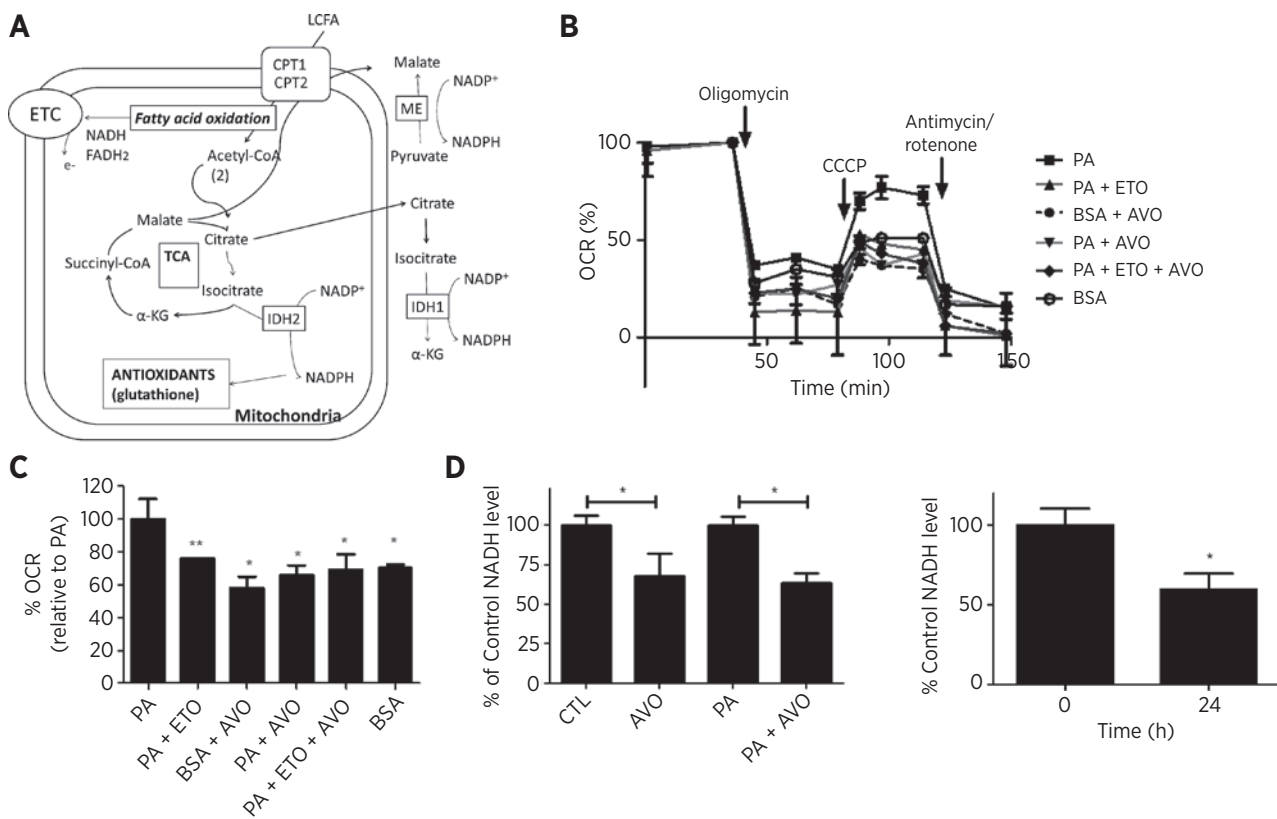


Figure 3.

Avocatin B inhibits fatty acid oxidation, resulting in decreased levels of NADH. A, illustration of fatty acid oxidation in mitochondria. Long-chain fatty acids (LCFA) enter the mitochondria via CPT1 for fatty acid oxidation to yield NADH and acetyl-CoA. Acetyl-CoA enters the TCA cycle to generate NADPH. ME, malic enzyme; IDH, isocitrate dehydrogenase; α -KG, α -ketoglutarate. B, oxidation of exogenous fatty acids was assessed by measuring the OCR in TEX cells treated with palmitate (175 μ mol/L), avocatin B (10 μ mol/L), avocatin B, and palmitate or palmitate and etomoxir (100 μ mol/L). Arrows, the time when oligomycin, CCCP, and antimycin/rotenone were added to the cells. Effects on fatty acid oxidation were measured with the Seahorse Bioanalyzer and quantified (C) by peak area after oligomycin and CCCP treatment, as described in the manufacturer's protocol and detailed in Materials and Methods. Data, percentage of OCR compared with palmitate-treated cells \pm SD. BSA was also used as a control. D, NADH was measured in TEX cells (left; $t = 3$ -5 hours) or primary AML cells (right; $n = 3$; $t = 24$ hours; results for OCI-AML2 cells are shown in Supplementary Fig. S9) using the commercially available Amplitude Fluorimetric Assay following treatment with avocatin B (10 μ mol/L), palmitate (175 μ mol/L), or avocatin B and palmitate according to the manufacturer's protocol. Data, percentage of NADH compared with vehicle control-treated cells \pm SD.

for m/z 285 and 287 were nearly identical between pure compound and the cellular fractions (pure avocatin B: 4.46 and 4.76; mitochondrial fraction: 4.46 and 4.78; cytosolic fraction: 4.46 and 4.78). As expected, avocatin B was not found in vehicle control-treated cells (Supplementary Fig. S7).

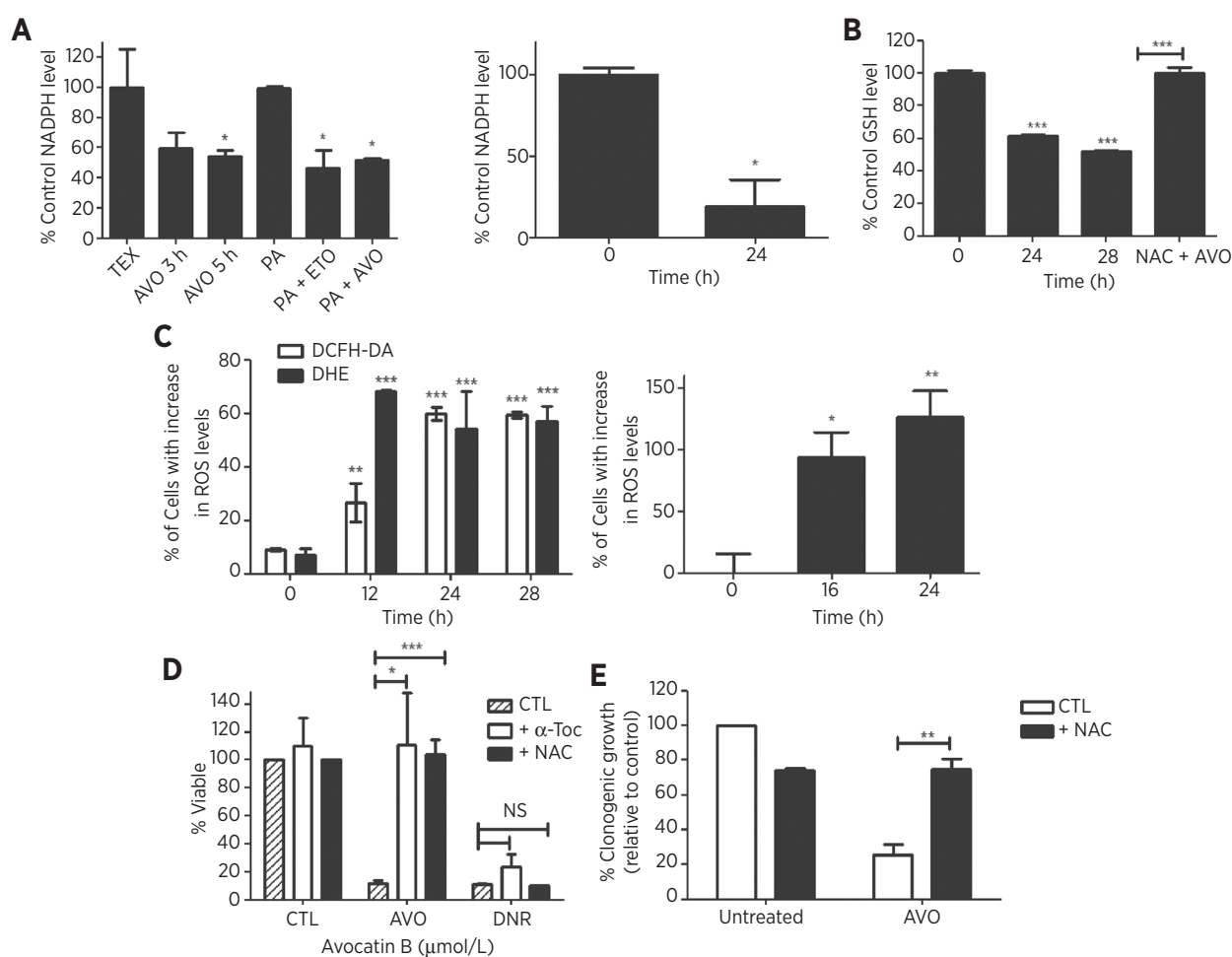
Lipids of 16 to 20 carbon length enter mitochondria by the activity of CPT1 (32). To determine the role of CPT1 in avocatin B-induced death, we blocked CPT1 chemically with etomoxir and genetically using RNA interference. Etomoxir concentrations that did not reduce viability (100 μ mol/L; Fig. 6A), abrogated avocatin B-induced cell death (Fig. 6B; $F_{5,17} = 94.45$; $P < 0.001$) and reductions in clonogenic growth (Fig. 6C; $F_{5,17} = 94.45$; $P < 0.001$). As a genetic approach, we generated cells with reduced CPT1 gene expression (mRNA: Fig. 6D, left; for protein see ref. 33). CPT1 knockdown cells were significantly less sensitive to avocatin B (Fig. 6D, middle; $F_{9,32} = 23.73$; $P < 0.001$) and were insensitive to avocatin B-induced reduction of NADPH (Fig. 6D, right; $F_{3,16} = 65.04$; $P < 0.001$). Together, these results show that avocatin B is

a lipid that localizes to the mitochondria and impairs fatty acid oxidation.

Discussion

A screen of a natural health product library identified avocatin B as a novel anti-AML agent. *In vitro* and preclinical functional studies demonstrated that it induced selective toxicity toward leukemia and LSCs with no toxicity toward normal cells. Mechanistically, we highlight a novel strategy to induce selective leukemia cell death, where mitochondrial localization of avocatin B inhibits fatty acid oxidation and decreases levels of NADPH, resulting in elevated ROS leading to apoptotic cell death.

Avocatin B targets leukemia over normal cells. We propose this specificity is related to the leukemia cells' altered mitochondrial characteristics, as a number of observations suggest avocatin B targets mitochondria. For example, (i) we directly show avocatin B

**Figure 4.**

Avocatin B decreased levels of NADPH and GSH and elevated ROS. A, NADPH was measured in TEX cells (left; $t = 3$ –5 hours) or primary AML cells ($n = 3$; $t = 24$ hours, right); results for OCI-AML2 cells are shown in Supplementary Fig. S9) using the commercially available Amplitude Fluorimetric Assay following treatment with avocatin B (10 $\mu\text{mol/L}$), palmitate (175 $\mu\text{mol/L}$), or etomoxir (100 $\mu\text{mol/L}$) according to the manufacturer's protocol. Data, a percentage of NADPH compared with vehicle control-treated cells \pm SD. B, GSH was measured in TEX cells in the presence or absence of NAC using a commercially available fluorimetric assay following treatment with avocatin B (10 $\mu\text{mol/L}$), according to the manufacturer's protocol. Data, percentage of GSH compared with vehicle control-treated cells \pm SD. C, ROS were measured in TEX cells (left) or primary AML cells ($n = 3$, right; results for OCI-AML2 cells is shown in Supplementary Fig. S9) treated with 10 $\mu\text{mol/L}$ avocatin B for increasing time by DHE and DCFH-DA by flow cytometry. Data, percentage of cells with increased ROS compared with vehicle control \pm SD from representative experiments. D, TEX cells were treated with 10 $\mu\text{mol/L}$ avocatin B in the presence or absence of NAC or α -Toc, which can neutralize ROS. Daunorubicin (DNR) was used as a negative control. Viability was measured by the Annexin V/PI assay; data, mean percentage of viable cells (i.e., Annexin V⁻/PI⁻) \pm SD from representative experiments. NS, nonsignificant. E, TEX cells were treated with 10 $\mu\text{mol/L}$ avocatin B in the presence or absence of NAC and colonies were counted as described in Materials and Methods. All experiments were performed three times in triplicate, and representative figures are shown. *, $P < 0.05$; **, $P < 0.01$; ***, $P < 0.001$.

accumulates in leukemia cell mitochondria using LC/MS; (ii) cells with significantly reduced mitochondria or (iii) lacking the enzyme that facilitates mitochondrial lipid transport, CPT1, are insensitive to avocatin B; (iv) chemical treatment with etomoxir, a CPT1 inhibitor, blocked avocatin B's activity; and (v) CPT1 only facilitates entry of lipids of avocatin B's size into mitochondria [e.g., 16–20 carbons (32); avocatin B:17 carbons (21)]. Compared with normal hematopoietic cells, leukemia cells contain higher mitochondrial mass (1) and depend on fatty acid substrates for survival (2). Thus, given this mitochondrial phenotype, we propose that avocatin B accumulates with greater concentration in leukemia over normal cells, thus conferring its increased toxicity toward leukemia cells.

Inhibition of fatty acid oxidation by avocatin B resulted in ROS-induced apoptosis. Apoptosis was characterized by the mitochondrial proteins cytochrome *c* and AIF, which are commonly released following ROS-induced increases in mitochondrial outer membrane permeability (34, 35). Inhibiting fatty acid oxidation by blocking CPT1 with etomoxir resulted in ROS-dependent death of glioma cells caused by reduced concentrations of intracellular antioxidants attributed to decreased NADPH (26). Similarly, we demonstrated that avocatin B-induced inhibition of fatty acid oxidation decreased NADPH and GSH levels and that antioxidant supplementation rescued cells from death. NADPH is used for catabolic processes in proliferating cells and is able to regenerate cellular antioxidants (i.e., convert oxidized GSH,

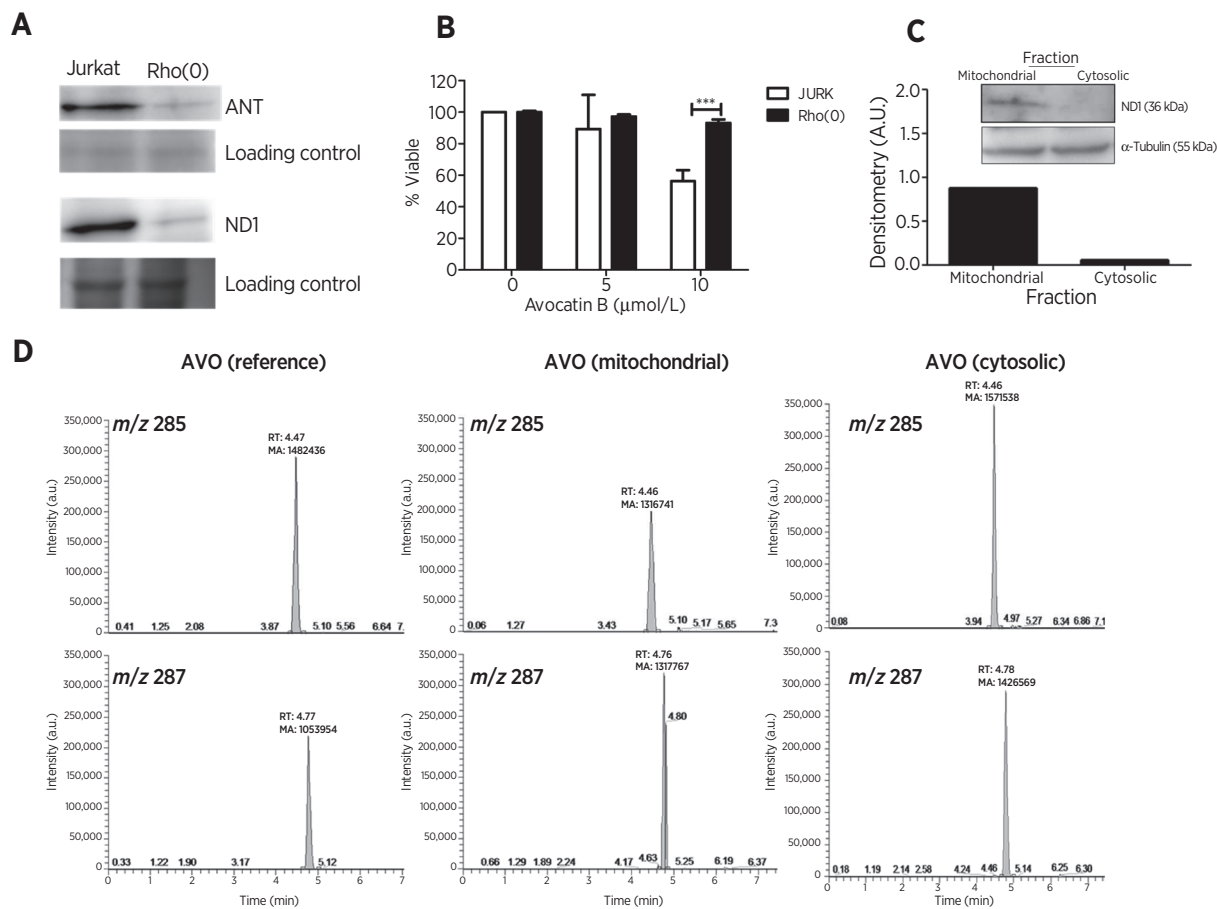


Figure 5. Mitochondria are functionally important for avocatin B-induced death. A, Jurkat T cells were cultured in 50 ng/mL of ethidium bromide, 100 mg/mL sodium pyruvate, and 50 $\mu\text{g/mL}$ uridine for 60 days to create Jurkat-Rho(O) cells, which lack functional mitochondria. To confirm that Jurkat-Rho(O) cells lack mitochondria, we measured the mitochondria-specific markers ANT and complex I (NDI) by Western blotting. B, avocatin B's activity was tested in cells with (JURK) and with reduced [Jurkat-Rho(O)] mitochondria. Viability was measured by the Annexin V/PI assay and flow cytometry; data, mean percentage of live cells (i.e., Annexin V⁻/PI⁻) \pm SD from representative experiments. C, mitochondrial and cytosolic fractions were collected, as outlined in Materials and Methods, and tested for purity by staining for the mitochondria-specific protein NDI. D, LC/MS chromatographs demonstrating the presence of avocatin B in the mitochondria and cytosol fractions of avocatin B-treated cells. All experiments were performed three times in triplicate, and representative figures are shown. ***, $P < 0.001$.

thioredoxins, and peroxiredoxins to their reduced equivalents), which counteract the detrimental effects of free radicals, including ROS; GSH specifically converts hydrogen peroxide to water (23, 36). Our observed NADPH decrease ($t = 5$ hours; Fig. 4A) preceded ROS elevation ($t = 12$ hours; Fig. 4C), further confirming the relationship between inhibition of fatty acid oxidation, NADPH, and ROS-dependent leukemia cell death. Of note, in our experiments, avocatin B accumulated in mitochondria to inhibit fatty acid oxidation and reduced NADPH at 10 $\mu\text{mol/L}$, whereas other studies used etomoxir, which blocks fatty acid entry into mitochondria and reduces NADPH at 100 $\mu\text{mol/L}$ (2) or 1,000 $\mu\text{mol/L}$ (26). Together, these results point to a mechanism in which avocatin B enters the mitochondria and potentially inhibits fatty acid oxidation, resulting in decreased NADPH and GSH leading to elevated ROS and apoptotic cell death.

Avocatin B is a 1:1 ratio of two 17-carbon lipids derived from methanol extracted from avocado pear seeds (*Persea gratissima*; ref. 20). Odd-numbered carbons are rare, not produced endogenously and obtained only from dietary sources (37, 38). More-

over, they are not efficiently or preferentially oxidized. For example, mice fed diets containing radiolabeled odd- and even-numbered fatty acids only accumulate odd-numbered fatty acids in adipose tissue (i.e., C15 and 17; ref. 39); odd-numbered fatty acids show consistent adipose accumulation (37, 40, 41). In humans, lipids of 13, 15, and 17 carbon lengths are used as serum and adipose tissue biomarkers of dietary fat intake, as these fatty acids are more slowly catabolized compared with even-numbered fatty acids (38, 42). Although they undergo the same pathway of oxidation, the terminal step of odd-numbered fatty acid oxidation produces 1 acetyl-CoA and 1 propionyl-CoA molecule, whereas even-numbered fatty acids produce 2 acetyl-CoA molecules (43). Propionyl-CoA can then be converted to methylmalonyl-CoA by propionyl-CoA carboxylase and vitamin B12, at the expense of 1 ATP, which, in turn, is converted to succinyl-CoA that can enter the TCA cycle (41). Because this alternate pathway requires energy and delays overall ATP production, the decreased metabolic activity (i.e., reduced acetyl-CoA production and/or decreased entry of fatty acid byproducts into

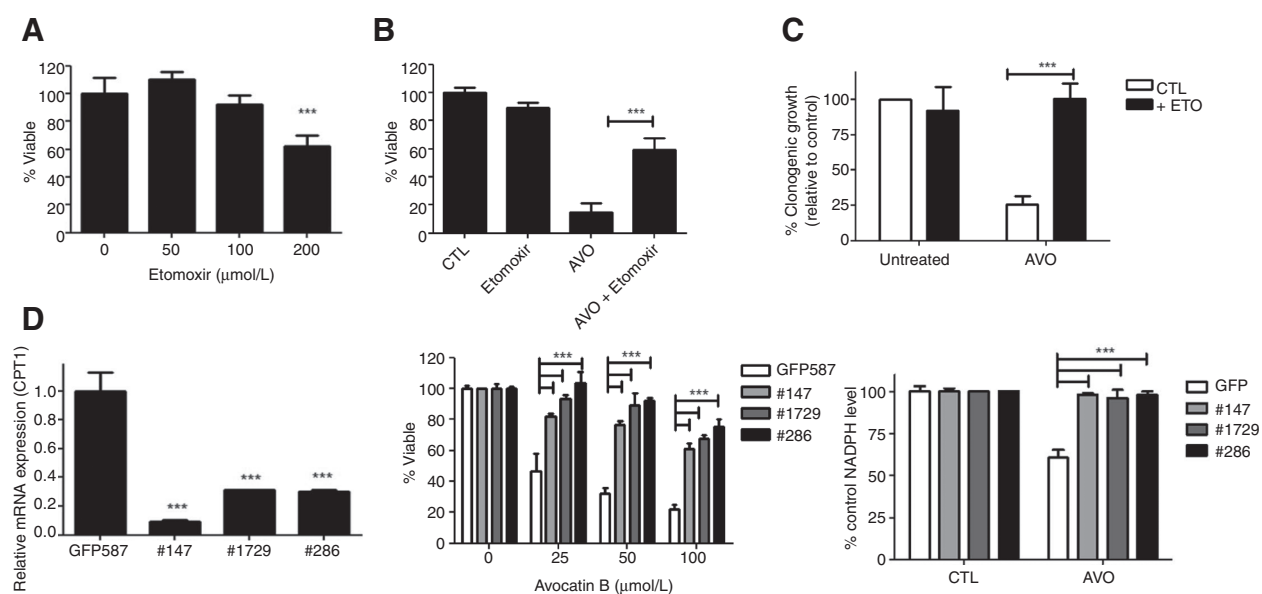


Figure 6.

CPT1 is functionally important for avocatin B-induced death. A, TEX cells were incubated with increasing concentrations of the CPT1 inhibitor etomoxir for 72 hours. B and C, avocatin B's (10 $\mu\text{mol/L}$) activity was tested using Annexin V/PI (B) or colony assays (C) in the presence of etomoxir (100 $\mu\text{mol/L}$; which does not impart toxicity). D, left, mRNA expression demonstrating knockdown of CPT1 in OCI-AML2 cells. Middle, avocatin B's activity was tested in CPT1 knockout cells. Right, NADPH was tested in CPT1 knockout cells following avocatin B (10 $\mu\text{mol/L}$) treatment. Data, percentage of NADPH relative to control. Unless otherwise noted, viability was measured by the Annexin V/PI assay and flow cytometry; data, mean percentage of live cells (i.e., Annexin V⁻/PI⁻) \pm SD from representative experiments. All experiments were performed three times in triplicate, and representative figures are shown. ***, $P < 0.001$.

the TCA cycle) likely explains our observed decrease in NAD and NADPH. As such, decreased levels of NADPH may not only result in elevated ROS, but also indicate a decrease in overall metabolic activity. Thus, a novel pathway by which fatty acid oxidation can be inhibited in leukemia cells is by the odd-numbered carbon lipid, avocatin B stalling or rendering less efficient the fatty acid oxidation pathway. This highlights a novel strategy to induce selective leukemia cell death by which preferential mitochondrial localization of avocatin B reduces leukemia cell metabolism and decreases NADPH, leading to ROS-mediated cell death.

Alternatively, mitochondrial accumulation of fatty acids could have lipotoxic effects. When in excess, fatty acids can accumulate inside the mitochondrial matrix where they are deprotonated, because of the proton gradient, creating fatty acid anions. These are converted by ROS into lipid peroxides that, in turn, cause damage to mitochondrial DNA, lipids, and proteins within the mitochondrial matrix (44). However, the generation of lipotoxic products requires ROS (45), therefore; avocatin B accumulation by itself would be insufficient to impart lipotoxicity. Thus, once inside the mitochondria, avocatin B or avocatin B derivatives may be converted to lipotoxic byproducts and contribute to death but only after sufficient ROS production (i.e., following avocatin B-induced inhibition of fatty acid oxidation). Thus, mitochondrial accumulation may contribute to death through lipotoxicity but this is not the underlying mechanism of avocatin B's activity.

Few compounds that inhibit fatty acid oxidation are currently approved for clinical use (23). CPT1 inhibitors, such as etomoxir and perhexiline, are associated with hepatotoxicity (46) and neurotoxicity (47), respectively, and are not approved for clinical use in North America. Other inhibitors, such as trimetazidine, which inhibits 3-ketoacyl-CoA thiolase, an enzyme involved in fatty acid

catabolism and ranolazine, which blocks late sodium currents, have had clinical success for the treatment of angina (48, 49). None of these compounds are approved for use in AML or other hematologic malignancies. Future studies are needed to assess avocatin B's pharmacology and pharmacokinetics; however, initial assessment of avocatin B's physicochemical properties suggests favorable tissue distribution. In particular, it possesses a high estimated partition coefficient ($\text{LogP} = 8.9$; ref. 21), indicating that it will accumulate in lipid-rich tissues such as adipose tissue and bone marrow. Given that LSCs reside in bone marrow, this could significantly enhance avocatin B's therapeutic efficacy. Nonetheless, future studies are needed to test the pharmacokinetics and safety of avocatin B in human trials.

In conclusion, avocatin B accumulated in mitochondria to inhibit fatty acid oxidation and decrease NADPH, resulting in ROS-mediated cell death characterized by the mitochondrial release of cytochrome *c* and AIF. Given the observed leukemia cell specificity, inhibiting fatty acid oxidation following avocatin B accumulation represents a novel therapeutic strategy that targets an important cellular pathway involved in leukemia cell activity.

Disclosure of Potential Conflicts of Interest

No potential conflicts of interest were disclosed.

Authors' Contributions

Conception and design: E.A. Lee, J.W. Joseph, A.D. Schimmer, P.A. Spagnuolo
Development of methodology: E.A. Lee, E. Boyaci, B. Bojko, S. Sriskanthadevan, J. Pawliszyn, J.W. Joseph, P.A. Spagnuolo
Acquisition of data (provided animals, acquired and managed patients, provided facilities, etc.): E.A. Lee, L. Angka, S.-G. Rota, T. Hanlon, A. Mitchell, X.M. Wang, M. Minden, A. Datti, J.L. Wrana, J.W. Joseph, J. Quadrilatero, P.A. Spagnuolo

Analysis and interpretation of data (e.g., statistical analysis, biostatistics, computational analysis): E.A. Lee, L. Angka, S.-G. Rota, A. Mitchell, E. Boyaci, A. Datti, J. Pawliszyn, J.W. Joseph, J. Quadrilatero, P.A. Spagnuolo

Writing, review, and/or revision of the manuscript: E.A. Lee, L. Angka, M. Gronda, M. Minden, A. Edginton, J.W. Joseph, A.D. Schimmer, P.A. Spagnuolo

Administrative, technical, or material support (i.e., reporting or organizing data, constructing databases): E.A. Lee, R. Hurren, M. Gronda, A.D. Schimmer, P.A. Spagnuolo

Study supervision: A.D. Schimmer, P.A. Spagnuolo

Acknowledgments

The authors thank Dr. John Dick for the generous gift of TEX cells.

References

1. Skrtic M, Sriskanthadevan S, Jhas B, Gebbia M, Wang X, Wang Z, et al. Inhibition of mitochondrial translation as a therapeutic strategy for human acute myeloid leukemia. *Cancer Cell* 2011;20:674–88.
2. Samudio I, Harmancey R, Fiegl M, Kantarjian H, Konopleva M, Korchin B, et al. Pharmacologic inhibition of fatty acid oxidation sensitizes human leukemia cells to apoptosis induction. *J Clin Invest* 2010;120:142–56.
3. Shipley JL, Butera JN. Acute myelogenous leukemia. *Exp Hematol* 2009;37:649–58.
4. Lowenberg B, Downing JR, Burnett A. Acute myeloid leukemia. *N Engl J Med* 1999;341:1051–62.
5. McDermott SP, Eppert K, Notta F, Isaac M, Datti A, Al-Awar R, et al. A small molecule screening strategy with validation on human leukemia stem cells uncovers the therapeutic efficacy of kintin riboside. *Blood* 2012;119:1200–7.
6. Spagnuolo PA, Hurren R, Gronda M, MacLean N, Datti A, Basheer A, et al. Inhibition of intracellular dipeptidyl peptidases 8 and 9 enhances parthenolide's anti-leukemic activity. *Leukemia* 2013;27:1236–44.
7. Spagnuolo PA, Hu J, Hurren R, Wang X, Gronda M, Sukhai MA, et al. The antihelminthic flubendazole inhibits microtubule function through a mechanism distinct from Vinca alkaloids and displays preclinical activity in leukemia and myeloma. *Blood* 2010;115:4824–33.
8. Sukhai MA, Prabha S, Hurren R, Rutledge AC, Lee AY, Sriskanthadevan S, et al. Lysosomal disruption preferentially targets acute myeloid leukemia cells and progenitors. *J Clin Invest* 2013;123:315–28.
9. Sachlos E, Risueno RM, Laronde S, Shapovalova Z, Lee JH, Russell J, et al. Identification of drugs including a dopamine receptor antagonist that selectively target cancer stem cells. *Cell* 2012;149:1284–97.
10. Angka L, Lee EA, Rota SG, Hanlon T, Sukhai M, Minden M, et al. Glucosylcholine increases cytosolic calcium to induce calpain-mediated apoptosis of acute myeloid leukemia cells. *Cancer Lett* 2014;348:29–37.
11. Abe Y, Sakairi T, Beeson C, Kopp JB. TGF-beta1 stimulates mitochondrial oxidative phosphorylation and generation of reactive oxygen species in cultured mouse podocytes, mediated in part by the mTOR pathway. *Am J Physiol Renal Physiol* 2013;305:F1477–90.
12. Dam AD, Mitchell AS, Rush JW, Quadrilatero J. Elevated skeletal muscle apoptotic signaling following glutathione depletion. *Apoptosis* 2012;17:48–60.
13. Owusu-Ansah E, Yavari A, Banerjee U. A protocol for *in vivo* detection of reactive oxygen species. 2008; doi:10.1038/nprot.2008.23.
14. Boyaci E, Sparham C, Pawliszyn J. Thin-film microextraction coupled to LC-ESI-MS/MS for determination of quaternary ammonium compounds in water samples. *Anal Bioanal Chem* 2014;406:409–20.
15. Boyaci E, Gorynski K, Rodriguez-Lafuente A, Bojko B, Pawliszyn J. Introduction of solid-phase microextraction as a high-throughput sample preparation tool in laboratory analysis of prohibited substances. *Anal Chim Acta* 2014;809:69–81.
16. McMillan EM, Graham DA, Rush JW, Quadrilatero J. Decreased DNA fragmentation and apoptotic signaling in soleus muscle of hypertensive rats following 6 weeks of treadmill training. *J Appl Physiol* 2012;113:1048–57.
17. Christensen ME, Jansen ES, Sanchez W, Waterhouse NJ. Flow cytometry based assays for the measurement of apoptosis-associated mitochondrial membrane depolarisation and cytochrome c release. *Methods* 2013;61:138–45.
18. Waterhouse NJ, Trapani JA. A new quantitative assay for cytochrome c release in apoptotic cells. *Cell Death Differ* 2003;10:853–5.
19. Warner JK, Wang JC, Takenaka K, Doulatov S, McKenzie JL, Harrington L, et al. Direct evidence for cooperating genetic events in the leukemic transformation of normal human hematopoietic cells. *Leukemia* 2005;19:1794–805.
20. Alves HM, Coxon DT, Falshaw CP, Godtfredsen WO, Ollis WD. The Avocatin—A new class of natural products. *Ann Braz Acad Sci* 1970;42:4.
21. ChemBank. 2014; Cited Sept 2014. <http://chembank.broadinstitute.org/chemistry/viewMolecule.htm?sessionId=9CC037B2065BFDE71429282-DD50A255?cbid=3198534>.
22. Konopleva M, Watt J, Contractor R, et al. Mechanisms of antileukemic activity of the novel Bcl-2 homology domain-3 mimetic GX15-070 (obatoclax). *Cancer Res* 2008;68:3413–20.
23. Carracedo A, Cantley LC, Pandolfi PP. Cancer metabolism: fatty acid oxidation in the limelight. *Nat Rev Cancer* 2013;13:227–32.
24. Heiden MG, Cantley LC, Thompson CB. Understanding the Warburg effect: the metabolic requirements of cell proliferation. *Science* 2009;324:1029–33.
25. Kirsch M, De Groot H. NAD(P)H, a directly operating antioxidant? *FASEB J* 2001;15:1569–74.
26. Pike LS, Smift AL, Croteau NJ, Ferrick DA, Wu M. Inhibition of fatty acid oxidation by etomoxir impairs NADPH production and increases reactive oxygen species resulting in ATP depletion and cell death in human glioblastoma cells. *Biochim Biophys Acta* 2011;1807:726–34.
27. Godbout JP, Berg BM, Kelley KW, Johnson RW. alpha-Tocopherol reduces lipopolysaccharide-induced peroxide radical formation and interleukin-6 secretion in primary murine microglia and in brain. *J Neuroimmunol* 2004;149:101–9.
28. Ferraro C, Quemeneur L, Prigent AF, Taverne C, Revillard JP, Bonnefoy-Berard N. Anthracyclines trigger apoptosis of both G₀-G₁ and cycling peripheral blood lymphocytes and induce massive deletion of mature T and B cells. *Cancer Res* 2000;60:1901–7.
29. Vejpongsa P, Yeh ETH. Topoisomerase 2 beta: a promising molecular target for primary prevention of anthracycline-induced cardiotoxicity. *Clin Pharmacol Ther* 2014;95:45–52.
30. Desjardins P, Frost E, Morais R. Ethidium bromide-induced loss of mitochondrial DNA from primary chicken embryo fibroblasts. *Mol Cell Biol* 1985;5:1163–9.
31. Hashiguchi K, Zhang-Akiyama QM. Establishment of human cell lines lacking mitochondrial DNA. *Methods Mol Biol* 2009;554:383–91.
32. Reddy JK, Hashimoto T. Peroxisomal beta-oxidation and peroxisome proliferator-activated receptor alpha: an adaptive metabolic system. *Annu Rev Nutr* 2001;21:193–230.
33. Sriskanthadevan S, Jeyaraju DV, Chung TE, Prabha S, Xu W, Skrtic M, et al. AML cells have low spare reserve capacity in their respiratory chain that renders them susceptible to oxidative metabolic stress. *Blood* 2015;125:2120–30.
34. Tomasello F, Messina A, Lartigou L, Schembri L, Medina C, Reina S, et al. Outer membrane VDAC1 controls permeability transition of the inner mitochondrial membrane in cellulose during stress-induced apoptosis. *Cell Res* 2009;19:1363–76.

Grant Support

This study was supported by grants from the Leukemia & Lymphoma Society of Canada and University of Waterloo (P.A. Spagnuolo); the Natural Sciences and Engineering Research Council of Canada (J. Quadrilatero and J. Pawliszyn); and the Canadian Institutes of Health Research (J.W. Joseph). A.D. Schimmer is a Leukemia and Lymphoma Society Scholar in Clinical Research.

The costs of publication of this article were defrayed in part by the payment of page charges. This article must therefore be hereby marked *advertisement* in accordance with 18 U.S.C. Section 1734 solely to indicate this fact.

Received September 11, 2014; revised March 17, 2015; accepted April 2, 2015; published online June 15, 2015.

35. Kroemer G, Galluzzi L, Brenner C. Mitochondrial membrane permeabilization in cell death. *Physiol Rev* 2007;87:99–163.
36. Vander Heiden MG, Cantley LC, Thompson CB. Understanding the Warburg effect: the metabolic requirements of cell proliferation. *Science* 2009;324:1029–33.
37. Campbell RG, Hashim SA. Deposition in adipose tissue and transport of odd-numbered fatty acids. *Am J Physiol* 1969;217:1614–8.
38. Wolk A, Furuheim M, Vessby B. Fatty acid composition of adipose tissue and serum lipids are valid biological markers of dairy fat intake in men. *J Nutr* 2001;131:828–33.
39. Gotoh N, Moroda K, Watanabe H, Yoshinaga K, Tanaka M, Mizobe H, et al. Metabolism of odd-numbered fatty acids and even-numbered fatty acids in mouse. *J Oleo Sci* 2008;57:293–9.
40. Pi-Sunyer FX. Rats enriched with odd-carbon fatty acids. Effect of prolonged starvation on liver glycogen and serum lipids, glucose and insulin. *Diabetes* 1971;20:200–5.
41. VanItallie TB, Khachadurian AK. Rats enriched with odd-carbon fatty acids: maintenance of liver glycogen during starvation. *Science* 1969;165:811–3.
42. Klein RA, Halliday D, Pittet PG. The use of 13-methyltetradecanoic acid as an indicator of adipose tissue turnover. *Lipids* 1980;15:572–9.
43. Berg JM, Tymoczko JL, Stryer L. *Biochemistry*. Certain fatty acids require additional steps for degradation. 5th ed. New York: W H Freeman; 2002. Available from: <http://www.ncbi.nlm.nih.gov/books/NBK22387/>.
44. Schrauwen P, Hesselink MK. Oxidative capacity, lipotoxicity, and mitochondrial damage in type 2 diabetes. *Diabetes* 2004;53:1412–7.
45. Schrauwen P, Schrauwen-Hinderling V, Hoeks J, Hesselink MK. Mitochondrial dysfunction and lipotoxicity. *Biochim Biophys Acta* 2010;1801:266–71.
46. Holubarsch CJ, Rohrbach M, Karrasch M, Boehm E, Polonski L, Ponikowski P, et al. A double-blind randomized multicentre clinical trial to evaluate the efficacy and safety of two doses of etomoxir in comparison with placebo in patients with moderate congestive heart failure: the ERGO (etomoxir for the recovery of glucose oxidation) study. *Clin Sci* 2007;113:205–12.
47. Ashrafian H, Horowitz JD, Frenneaux MP. Perhexiline. *Cardiovasc Drug Rev* 2007;25:76–97.
48. Passeron J. [Effectiveness of trimetazidine in stable effort angina due to chronic coronary insufficiency. A double-blind versus placebo study]. *Presse Med* 1986;15:1775–8.
49. Aldakkak M, Stowe DF, Camara AK. Safety and efficacy of ranolazine for the treatment of chronic angina pectoris. *Clin Med Insights Ther* 2013;2013:1–14.